

An alternative kinetic model of the iodide-iodate reaction for its use in micromixing investigations

Arturo N. Manzano Martínez,[†] A. Sander Haase,[‡] Melissa Assirelli,[‡] and John van der Schaaf^{*,†}

[†]Laboratory of Chemical Reactor Engineering, Department of Chemical Engineering and Chemistry, Eindhoven University of Technology, P.O. Box 513, 5600 MB Eindhoven, The Netherlands

[‡]Nouryon, Zutphenseweg 10, P.O. Box 10, 7400 AA Deventer, The Netherlands

E-mail: j.vanderschaaf@tue.nl

Abstract

The Villiermaux-Dushman method, one of the most extensively used test reaction systems for micromixing characterization, has been widely criticized for years due to uncertainties regarding the incomplete dissociation of sulfuric acid and the proposed kinetic study by Guichardon et al. In this work, a renewed study of the kinetics of the iodide-iodate reaction is presented, using perchloric acid to avoid issues concerning incomplete acid dissociation. The experimental results are in good agreement with the fifth order rate law for the iodide-iodate reaction. The reaction rate coefficient strongly depends on the ionic strength and can be modeled with a Davies-like equation. When implemented in the incorporation model, the kinetic model presented in this study can be used to estimate micromixing times that are in line with the theoretical

engulfment time. This is observed in two different reactors with low and high intensity of mixing: an unbaffled stirred vessel and a rotor-stator spinning disc reactor. The results from the latter are also compared with the second Bourne reaction, giving very similar micromixing times. The use of sulfuric acid in combination with the kinetic model from Guichardon et al. also provides micromixing times of the same order of magnitude; presumably their kinetic model indirectly accounts for the second proton dissociation rate in the overall reaction rate coefficient. The kinetic model presented in this study in combination with perchloric acid is suggested as an alternative to characterize micromixing behavior.

1 Introduction

For the chemical industry, the understanding of mixing plays a crucial role when fast complex chemical reactions take place: it can affect selectivity and yield,¹ the size of crystals and precipitates,² or the molecular weight of polymers.³

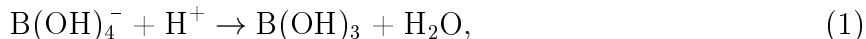
5 For these reasons, micromixing characterization has been an important research topic in the last few decades, both to its relevance in the design and scale-up of new equipment,⁴⁻⁹ as well as to understand and optimize the operational conditions and feed streams in traditional reactors.¹⁰⁻¹⁴

A heuristic definition of mixing is the homogenization of a system: the reduction of
10 gradients of concentration, temperature, phases, and so on. Thus, micromixing is commonly defined as the homogenization of the system at the smallest scale where reaction occurs.¹⁵ This process has a characteristic time, commonly called the micromixing time,¹⁶ and it can define the product distribution of fast competitive-consecutive or parallel-competitive reactions.¹⁷

15 When Direct Numerical Simulations are difficult to perform due to complex geometries or complex hydrodynamic conditions, test reactions and mixing models are used to measure qualitatively and quantitatively the micromixing time in chemical reactors.

One of the most extensively employed test reaction systems is the Villiermaux-Dushman system, developed in the 1990's¹⁸ and since then used to characterize both traditional and novel reactors. Another test reaction that is used in micromixing investigations is the second Bourne reaction,¹⁹ which involves the simultaneous diazo-coupling of 1-naphthol and 2-naphthol with diazotized sulfanilic acid in a basic environment. Although the kinetics of the second Bourne reaction have been carefully investigated and revised,^{5,19,20} the Villiermaux-Dushman method has been preferred among researchers for being experimentally and analytically easier to perform.

The complete experimental method of the Villiermaux-Dushman system^{21,22} is briefly summarized as a slow addition of a proton source to a bulk solution. Depending on the micromixing efficiency it can favor one of the two possible reactions: the nearly instantaneous neutralization of a buffer containing borate ions,¹



or the iodide-iodate reaction



To evaluate the micromixing efficiency in process equipment, typically the segregation index X_S is used, which represents the selectivity towards the undesired product Y :

$$X_S = \frac{Y}{Y_{ST}}. \quad (3)$$

¹In micromixing investigations, orthoboric acid and borate ion are commonly represented as H_3BO_3 and H_2BO_3^- , respectively. However, orthoboric acid shows Lewis acidity, accepting a hydroxy group.²³ It is more appropriate to represent them as B(OH)_3 and B(OH)_4^- .

Y is the ratio of acid mole number consumed by iodide-iodate reaction,

$$Y = \frac{2(n_{\text{I}_2} + n_{\text{I}_3^-})}{n_{\text{H}^+}}. \quad (4)$$

Y_{ST} is the value of Y assuming an infinitely slow micromixing process, leading to a situation
35 in which the acid is consumed in proportion to the local concentration of borate ions and
iodate ions:

$$Y_{ST} = \frac{6[\text{IO}_3^-]_0}{6[\text{IO}_3^-]_0 + [\text{H}_2\text{BO}_3^-]_0}. \quad (5)$$

When perfect mixing is achieved, no iodine is produced and $X_S = 0$. On the other
hand, under a situation where complete segregation occurs $X_S = 1$. In this way, experimen-
tally obtained values of X_S can indicate the micromixing efficiency at different operational
40 conditions.

This method is very sensitive to mixing effects and produces reproducible results. By
using the same concentration set, one can rank different mixers and devices. However,
to quantitatively determine micromixing times, sufficient information about the kinetics
is required, and for some years there has been controversy on whether the kinetic model
45 proposed by Guichardon et al.²⁴ for the iodide-iodate reaction is accurate enough to quantify
micromixing times.^{25,26}

In 2000, Guichardon et al.²⁴ published a kinetic model to determine micromixing times
using the Villermaux-Dushman method. In their work, previous kinetic studies were sum-
marized and discussed, partial reaction orders were determined, and an empirical model for
50 the reaction rate coefficient k with a dependency on the ionic strength I_s was proposed:

$$r = -\frac{d[\text{IO}_3^-]}{dt} = k[\text{IO}_3^-][\text{I}^-]^2[\text{H}^+]^2, \quad (6)$$

with

$$I_s < 0.166, \quad \log_{10}(k) = 9.281 - 3.664\sqrt{I_s}, \quad (7)$$

$$I_s > 0.166, \quad \log_{10}(k) = 8.383 - 1.511\sqrt{I_s} + 0.237I_s. \quad (8)$$

The salt used to study the effects of ionic strength was potassium sulfate. In combination with sulfuric acid as the proton source, this led to a buffer-like situation, as others already discussed.²⁷ The sulfate ions, acting as a weak base, could catch and later release protons, leading to slower reaction rates. In other words, this apparent reaction was a combination of
55 the iodide-iodate reaction plus the equilibrium reaction of the protonation and deprotonation of the sulfate species.

In 2016, a revision of the kinetics²⁸ took place, acknowledging the above mentioned effect. The revision indicated that the second dissociation of the acid should be included in the model and an updated model for the reaction rate coefficient was presented. However,
60 no information about the kinetic rates of the dissociation constant were given, and the recalculated reaction rate constant increased with increasing ionic strength, a phenomenon unlikely to occur in aqueous solutions at moderate ionic strengths.²⁹

As first discussed in 2010 by Kölbl et al.,³⁰ and later explored by Baquerio et al.³¹ and Wenzel et al.,³² the use of a strong monoprotic acid such as perchloric acid could
65 be an alternative to avoid the uncertainties due to the incomplete dissociation of sulfuric acid. However, whether the kinetics of the iodide-iodate depend on the used acid was not confirmed.

The Dushman reaction was studied also by Schmitz et al.³³⁻³⁷ However, their work focused on understanding other reaction systems: the oscillating Bray-Liebhafsky reaction,
70 the Briggs-Rausher reaction, and the reaction mechanisms of other iodine-related reactions. Their most recent kinetic model,³⁷ which is limited to low values of ionic strength ($I_s < 0.2$ M), has not been used for micromixing investigations.

The purpose of this work, of which its preliminary results were presented during the AIChE Annual Meeting 2019,³⁸ was to determine the reaction rate of the iodide-iodate
75 reaction when using perchloric acid as the proton source, and to propose a kinetic model that allows quantification of micromixing times when using the Villermaux-Dushman method. Micromixing experiments were carried out in a rotor-stator Spinning Disc Reactor (rs-SDR) and in a Stirred Vessel (SV) using the Villermaux-Dushman method to verify the suitability of the proposed kinetic model in equipment with different mixing intensities. Furthermore, a
80 diluted concentration set for the Villermaux-Dushman system using perchloric acid was used to analyze its variability under similar hydrodynamic conditions. The results were compared with those obtained using the original Villermaux-Dushman method with sulfuric acid using the kinetic model proposed by Guichardon et al.²⁴ Finally, the results were compared to estimated micromixing times obtained with the second Bourne reaction system to confirm
85 the validity of the proposed kinetic model for the Villermaux-Dushman system.

2 Materials and methods

2.1 Kinetics of the iodide-iodate reaction

The experimental setup involved a batch reactor, represented schematically in Figure 1. The small jacketed glass reactor had an inner diameter of $D_{batch} = 2.5 \times 10^{-2}$ m, an inner height
90 of $H_{batch} = 2 \times 10^{-1}$ m, an outer diameter of $D_{jacket} = 3.5 \times 10^{-2}$ m, and total height of $H_{jacket} = 2.05 \times 10^{-1}$ m. Through the jacket, cooling liquid was recirculated to keep the reactor at a constant temperature of 20 °C using a Lauda Ecoline RE104 cooling bath.

Depending on the investigated parameter, the batch reactor was loaded with 50×10^{-3} L solution containing potassium iodide (VWR Chemicals, $\geq 99\%$), potassium iodate (Merck,
95 98%), and sodium perchlorate monohydrate (Alfa Aesar, $\geq 99.0\%$) to tune the ionic strength to the desired values. The proton source, perchloric acid (VWR Chemicals, 65%), was added to the reactor in pulses, using a 1×10^{-3} L syringe. During every experiment, the reactor

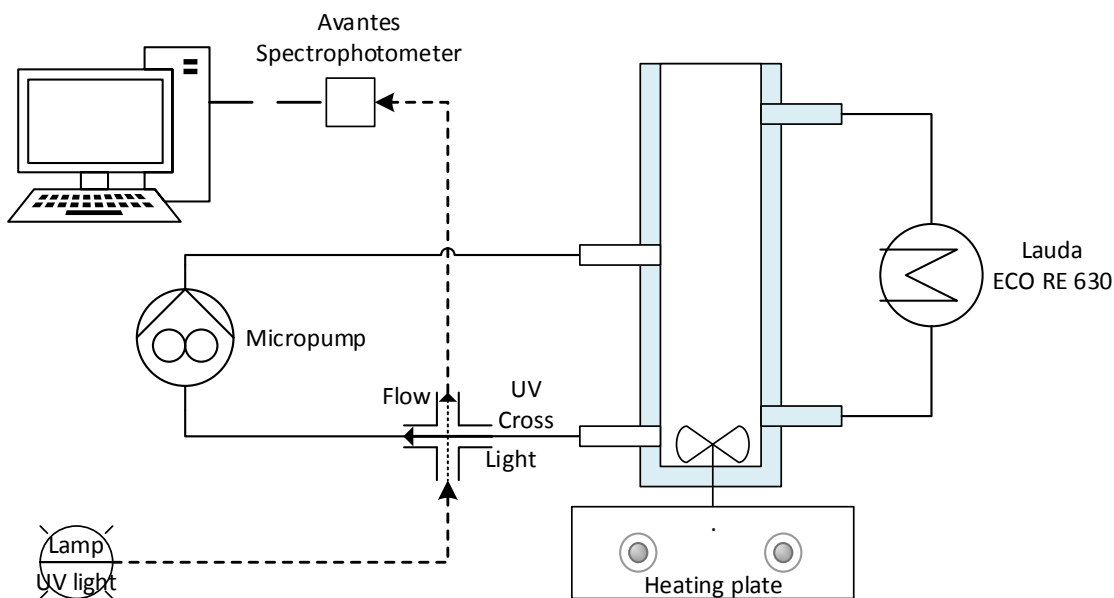


Figure 1: Schematic representation of the batch setup used for the kinetic study

was stirred using a small magnetic stirrer at constant speed, which was carefully selected to avoid macromixing effects. All experiments were performed at least three times.

100 Table 1 summarizes the concentrations (after mixing) used for each investigated parameter. The concentrations were carefully selected, based on preliminary data, to maximize sensitivity of the reaction rates and avoid saturation of the employed analytical method (spectrophotometry). Fresh solutions were daily prepared using demineralized water, stripped with nitrogen gas.

105 The reactor included a small recirculation line with an in-line flow cell attached for real-time spectroscopy measurements. For each experiment, the signal at a wavelength of 353 ± 1 nm was recorded (integration time 1.05 ms) with an AvaSpec-2048 spectrophotometer (Avantes) using the Avalight DH-S (Avantes) as a light source. The flow in the recirculation line, with an estimated volume of 0.6×10^{-3} L (negligible compared to the contents of the reactor), was kept at a constant rate of 8.3×10^{-3} L s⁻¹ using a gear pump ISMATEC REGLO-Z Digital equipped with pump-head Z-186.

110

Table 1: Set of concentrations according to the investigated parameter. Each column (2 to 5) shows the investigated parameter, with the corresponding set of concentrations of the reagents in the rows below.

	Investigated parameter			
	IO_3^-	I^-	H^+	I_s
$[\text{KIO}_3], \text{M}$	$4.0 - 50.0 \times 10^{-6}$	2.5×10^{-5}	2.5×10^{-5}	2.5×10^{-5}
$[\text{KI}], \text{M}$	5.0×10^{-3}	$2.5 - 10.0 \times 10^{-3}$	1.0×10^{-2}	1.0×10^{-2}
$[\text{HClO}_4], \text{M}^a$	1.0×10^{-3}	1.0×10^{-3}	$1.9 - 38.0 \times 10^{-4}$	1.0×10^{-3}
$[\text{NaClO}_4], \text{M}$	0.0, 0.1, 1.0	0.0, 0.1, 1.0	0.0, 0.1, 1.0	$1.1 - 100.0 \times 10^{-2}$

^a For the experiments carried out at 1.0 M ionic strength, the concentration of acid was doubled to 2.0×10^{-3} M to keep the reaction time under 300 seconds.

2.2 Analysis of the kinetic data

The quasi-instantaneous equilibrium reaction of iodide ions and iodine to form tri-iodide ions³⁹ is a key feature for studying the kinetics of the iodide-iodate reaction, provided that

115 an excess of iodide ions is present at all times:



The temperature-dependent equilibrium constant K_{eq} ,

$$K_{eq} = \frac{[\text{I}_3^-]}{[\text{I}_2][\text{I}^-]}, \quad (10)$$

is defined by the following expression:⁴⁰

$$\log_{10} K_{eq} = \frac{555}{T} + 7.355 - 2.575 \log_{10} T. \quad (11)$$

A concentration profile of tri-iodide was obtained using the signal from the spectrophotometer using the Beer-Lambert law. Under the studied conditions the value of the absorbance at 353 nm was always in the linear range.

120

By adding a pulse of 1×10^{-3} L of diluted methylene blue (VWR Chemicals, 1% w/v aq. soln.) to the reactor containing 50×10^{-3} L of water, and recording the signal from the

spectrophotometer at a wavelength of 665 ± 1 nm, the macromixing time (95% homogenization) was determined to be always less than 5 s. To determine the reaction rate coefficient k , the first 7 s after the reaction was started were not considered.

2.3 Fitting procedure

For each experiment, the tri-iodide concentration $C_{I_3^-}$ as obtained from the absorbance measurements was recorded as a function of time t . Recognizing that the limiting reagent² for the iodine formation is potassium iodate⁴¹ and knowing the initial concentration of the reagents for each experiment (Table 1), the mass balance closed. That provided a concentration profile of all the species. These concentration profiles were used to model the system as a batch reactor using MATLAB (version 2017b).

The set of ordinary differential equations that describes the concentration over time in a batch system for species i takes the form of

$$\frac{dC_i}{dt} = C_i \pm r, \tag{12}$$

where the experimentally obtained concentration profiles were used to fit the reaction rate coefficient k as shown in Equation 6. This fitting was performed using the built-in function ‘fminsearch’, and an objective function defined as the sum of squared estimate of errors (SSE), i.e.:

$$\text{SSE} = \sum (C_{I_3^-,exp} - C_{I_3^-,mod})^2, \tag{13}$$

where the suffix *exp* stands for experimental, and *mod* for modeled.

Typical tri-iodide concentration profiles and their fitted curves can be found in the Supplementary information.

At least three experiments were performed for a given set of concentrations, and the average values of k were compared against the ionic strength to obtain a correlation. The

²In iodometry this redox reaction proceeds by iodate ions oxidizing the iodide ions in acidic environment.

fitting was performed using the ‘Curve Fitting Toolbox’ from MATLAB (version 2017b), to
145 allow the use of custom equations. A nonlinear least-squares fitting was performed, and the
fit options were changed to increase the maximum number of function evaluations to 6000,
maximum number of iterations to 4000, while the termination tolerance on function value
and termination tolerance on x were both decreased to 1.0×10^{-12} .

2.4 Second Bourne reaction

150 As mentioned in the introduction, a very well established test reaction for micromixing
characterization is the second Bourne reaction, also referred to as diazocoupling of naph-
thols. Originally consisting of the diazo-coupling of 1-naphthol with the diazonium salt of
sulfanilic acid,²⁰ this method was later extended to include the competitive azo-coupling of
2-naphthol to characterize devices with high energy input.¹⁹ The reaction scheme follows the
155 competitive-consecutive and parallel-competitive second order reactions:



and



160 where $A1$ stands for 1-naphthol, $A2$ is 2-naphthol, B represents diazotized sulfanilic acid, $p - R$ and $o - R$ are the monoazo substituted products in the para and ortho positions respectively, S is the bisazo product, and finally Q is the monoazo product of $A2$.

The kinetic rate coefficients of these reactions were measured (Bourne et al.)¹⁹ in a stopped-flow apparatus, at a temperature of 298 K, pH of 9.9 (sodium carbonate / sodium bicarbonate buffer) and ionic strength $I_s = 0.444$ M. The values for the reaction rate coefficients from Equations 14 - 18 are $k_1o = 9.2100 \times 10^5 \text{ M}^{-1}\text{s}^{-1}$, $k_1p = 1.2238 \times 10^7 \text{ M}^{-1}\text{s}^{-1}$, $k_2p = 1.8350 \times 10^3 \text{ M}^{-1}\text{s}^{-1}$, $k_2o = 2.2250 \times 10^4 \text{ M}^{-1}\text{s}^{-1}$, and $k_3 = 1.2450 \times 10^5 \text{ M}^{-1}\text{s}^{-1}$, respectively.

Under perfect micromixing conditions, only the fastest reaction represented by Equation 170 15 would proceed. However, under a mixing controlled regime the other slower reactions also proceed, forming products S and Q . Thus, the product distribution is reflected by the Segregation Index X'_S for the competitive-consecutive system

$$X'_S = \frac{2[S]}{[o - R] + [p - R] + 2[S] + [Q]}, \quad (19)$$

and X_Q for the parallel-competitive part

$$X_Q = \frac{[Q]}{[o - R] + [p - R] + 2[S] + [Q]}. \quad (20)$$

In high-intensity equipment such as the rs-SDR, the bisazo product S is barely formed 175 and only X_Q becomes relevant.¹⁹

2.5 Micromixing experiments

To validate the results from the kinetic study, micromixing experiments were performed using two setups: a 5 L Stirred Vessel (SV) and a rotor-stator Spinning Disc Reactor (rs-SDR). Furthermore, the Villermaux-Dushman experiments were carried out with both perchloric 180 acid and sulfuric acid. Additionally, a diluted concentration set of the Villermaux-Dushman

system and the second Bourne reaction were performed in the rs-SDR to verify the estimation of micromixing times in high-intensity mixing equipment. If the hydrodynamics define the mixing environment, the micromixing times should be

The concentration sets used are shown in Table 2. Fresh solutions were prepared before the experiments to avoid degradation of the reagents.

Table 2: Set of concentrations used in the micromixing experiments.

Villermaux-Dushman			
		Typical	Diluted
Bulk solution	[B(OH) ₃], M	0.1818	0.012
	[NaOH], M	0.0909	0.006
	[KI], M	0.0120	0.0117
	[KIO ₃], M	0.0023	0.0023
Acid injection	[HClO ₄], M	1.0400	0.104
	[H ₂ SO ₄], M	0.5300	
Second Bourne reaction			
Bulk solution	[Na ₂ CO ₃], M	0.1110	
	[NaHCO ₃], M	0.1110	
	[1-Naphthol], M	0.0012	
	[2-Naphthol], M	0.0036	
Acid injection	[Diazotized Sulfanilic Acid], M	0.5300	

185

A schematic representation of the rs-SDR is given in Figure 2. Different than in a previous publication,⁶ for this study the experiments were carried out in semi-batch operation. A 5 L bulk solution was charged to a tank that fed the rs-SDR. The outflow was returned to the tank, and the method of successive injections was adopted.²¹ At the rim of the disc,
 190 the zone with the highest local energy dissipation rate in the reactor, 10×10^{-3} L of acid was slowly injected at a flowrate of 3.33×10^{-5} L s⁻¹ to ensure being in the micromixing regime. In-line measurements of the absorbance were recorded from the inlet and outlet of the reactor (Dual channel Avaspec-2048-2-USB2 spectrophotometer (Avantes), Avalight DH-S light (Avantes)). As soon as the two signals for absorbance overlapped, steady-state was
 195 achieved and the rotational speed was modified. The segregation index X_S was calculated using Equation 3.

The experiments carried out in the unbaffled Stirred Vessel (SV) were performed in the

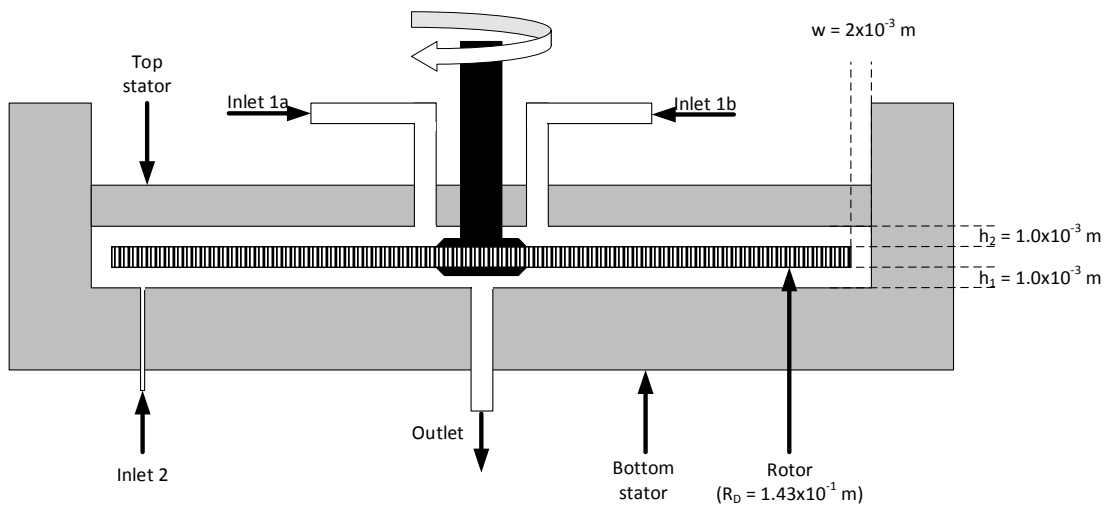


Figure 2: Schematic representation of the rotor-stator spinning disc reactor used for the micromixing experiments.

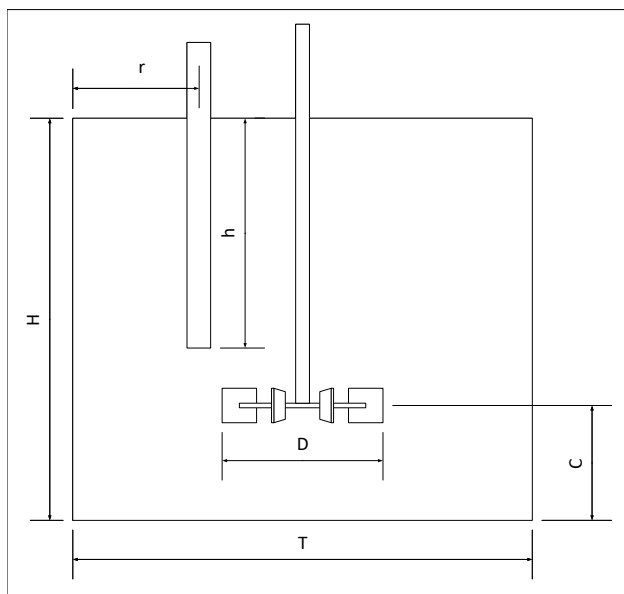


Figure 3: Schematic representation of the Stirred Vessel used for the micromixing experiments.

same tank that fed the rs-SDR. Figure 3 shows a schematic representation. A six blade
 Rushton Turbine with a diameter of $D = 7 \times 10^{-2}$ m with a blade height of $B = 1.5 \times 10^{-2}$
 200 m was introduced into the 5.5 L tank of diameter $T = 2 \times 10^{-1}$ m and height $H = 1.75 \times 10^{-1}$
 m. The stirrer was located at a distance $C = 5 \times 10^{-2}$ m from the bottom of the vessel. 4 L
 bulk solution was loaded to the tank, and 5×10^{-3} L of acid was injected also at a flowrate
 of 3.33×10^{-5} L s⁻¹. The acid was fed through a 1/8" standard stainless steel pipe located
 very close to the tip of the impeller, at a distance $r = 6 \times 10^{-2}$ m from the wall of the tank
 205 and height $h = 1 \times 10^{-1}$ m from the top of the tank. The absorbance signal was recorded
 with the same spectrophotometer that was used with the rs-SDR.

To perform the diazocoupling of 1-naphthol and 2-naphthol,¹⁹ 1 L of bulk solution was
 used, and 20×10^{-3} L of the diazotized sulfanilic acid was injected at a flowrate of 3.33×10^{-5}
 L s⁻¹. After the injection was completed, a 1×10^{-3} L sample of the final solution was diluted
 210 using 9×10^{-3} L of a sodium carbonate and sodium bicarbonate buffer to allow spectropho-
 tometric measurement using spectrophotometer UV-2501PC (Shimadzu Corporation). The
 product distribution was determined using the values for the extinction coefficients of all
 species as presented in Ref.^{19,20} The segregation index X_Q was calculated using Equation 20.

2.6 Local energy dissipation rate

215 According to turbulence theory,⁴² kinetic energy is transferred from the larger scales in the
 flow field to the smallest vortices where energy is dissipated. Following the law of conservation
 of energy, the mechanical energy that the Rushton turbine or the rotor from the rs-SDR exerts
 into the reactor contents must be dissipated in the smallest eddies in the turbulent field by
 viscous forces. The lengthscale of the smallest eddies is defined by dimensional analysis
 220 as $\eta_K = (\nu^3/\epsilon)^{(1/4)}$. These eddies have a turnover time of $\tau_K = (\nu/\epsilon)^{(1/2)}$. Bałdyga and
 Bourne⁴³ found that the hydrodynamically most active eddies (having the highest vorticities)
 have a size of approximately $11.5\eta_K$ and a characteristic time of $12.7\tau_K$, and reactive mixing
 is defined by engulfment, deformation and diffusion of these eddies.⁴⁴

In unbaffled stirred vessels, the average energy dissipation rate $\epsilon_{average}$ can be estimated
225 from:

$$\epsilon_{average} = \frac{P}{\rho V}, \quad (21)$$

using the Power Number Po from:⁴⁵

$$Po = \frac{P}{\rho N^3 D^5} = 0.8. \quad (22)$$

The local energy dissipation rate depends on the location of the feed point, and is typically
related to the average value with a proportionality constant ϕ . Typical values for positions
close to the impeller range from 20 to 150. In this case a value of $\phi = 35$ was assumed, in
230 agreement with other studies.^{10,45-49}

For the rs-SDR, the averaged energy dissipation rate was directly measured from the
motor using the characteristic torque $M_c = 9.4 \text{ Nm A}^{-1}$, the rotational speed ω and the
nominal current I :

$$\epsilon_{average} = \frac{\omega I M_c}{\rho V}, \quad (23)$$

and the local energy dissipation rate can be correlated by a momentum balance using the
235 correlations from Daily and Nece⁵⁰ for the frictional torque. An explanation of the procedure
is presented by de Beer et al.⁵¹ In this case, the proportionality value corresponding to the
injection zone is $\phi = 2.19$.

3 Results

3.1 Kinetic study

240 Assuming that the fifth order rate law is the best description of the iodide-iodate reaction,
the reaction rate coefficient k obtained from the fitting procedure should only depend on the
ionic strength, whilst variations in the reactant concentrations should not affect its value.

Figure 4 summarizes the observed reaction rate coefficients obtained for the different concentration sets described in Table 1. These results show that k strongly depends on the ionic strength. The concentration of the reagents at constant ionic strength has no influence on the observed reaction rate coefficient, which means that the fifth order rate law is valid and that the partial reaction orders for the involved species are also correct. The dependency on the ionic strength is attributed to the nature of the mixture, being an aqueous electrolyte solution.²⁹

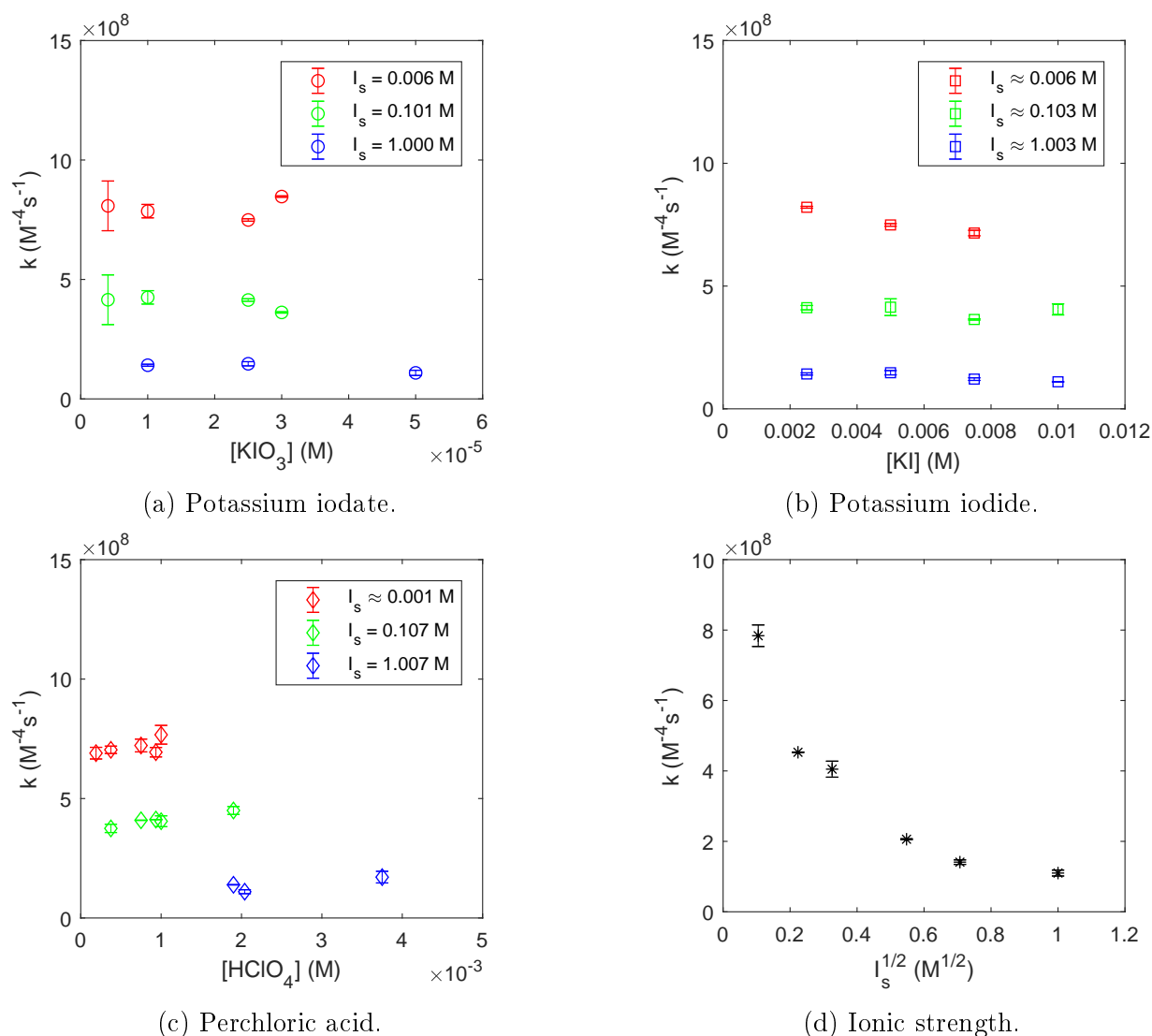


Figure 4: Reaction rate coefficient k as function of the specified parameters for the experimental conditions summarized in Table 1. Error bars represent the standard deviation for at least three experiments.

250 Rewriting Equation 6 into an expression that includes the activity of the species (a_i) instead of their concentration leads to:

$$r = k_0 a_{\text{IO}_3^-} a_{\text{I}^-}^2 a_{\text{H}^+}^2. \quad (24)$$

The activity of each species is related to the concentration via the activity coefficient γ_i , i.e.

$$r = k_0 (\gamma_{\text{IO}_3^-} [\text{IO}_3^-]) (\gamma_{\text{I}^-} [\text{I}^-])^2 (\gamma_{\text{H}^+} [\text{H}^+])^2. \quad (25)$$

For the sake of simplicity, an uniform activity coefficient γ is used. Additionally, it is 255 assumed that the activity coefficient is well represented by a Davis-like equation as the one proposed by Bromley et al.:^{29,52}

$$\log_{10}(\gamma) = -0.51 \left(\frac{\sqrt{I_s}}{1 + \sqrt{I_s}} \right) + \frac{(0.06 + 0.6B_m) I_s}{(1 + 1.5I_s)^2} + B_m I_s. \quad (26)$$

That means that the observed reaction rate coefficient from the experiments is in fact the product of a value for the reaction rate coefficient at infinite dilution, k_0 , and the activity coefficients:

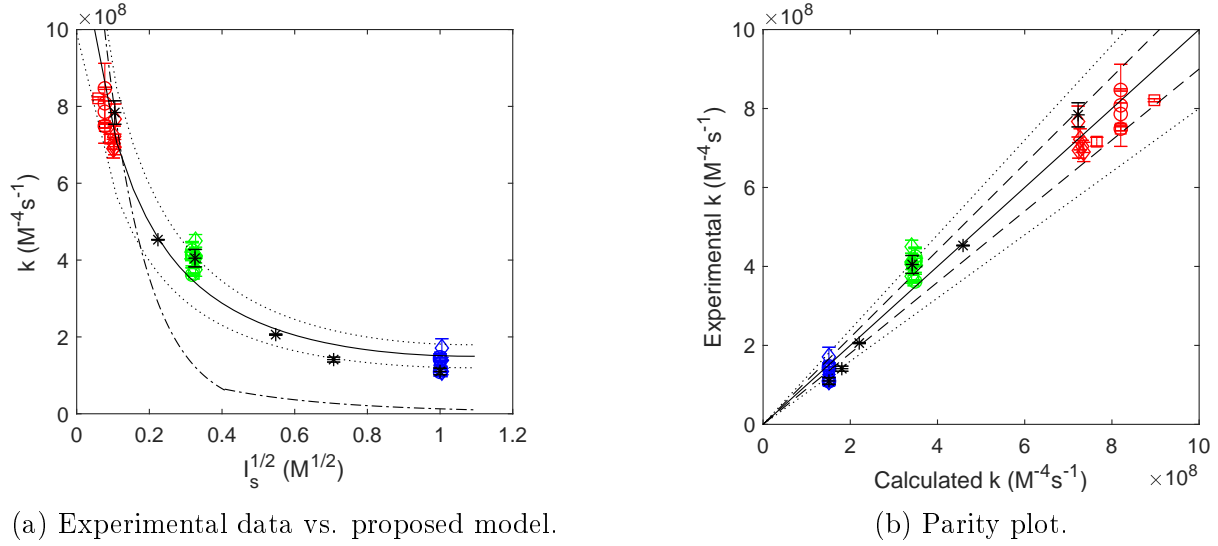
$$k = k_0 \gamma^5. \quad (27)$$

260 From the experimental data, k_0 and the parameter B_m from Equation 26 were fitted as a function of ionic strength. The results are presented in Table 3.

Figure 5a shows that the proposed kinetic model describes the experimentally determined reaction rate coefficients very well. The parity plot in Figure 5b shows that the model predicts the reaction rate coefficient within 20% accuracy for most of the experiments.

Table 3: Fitted coefficients for the estimation of γ and k .

Parameter	Value	95% confidence interval
$B_m, \text{L mol}^{-1}$	0.05722	(0.04158, 0.07286)
$k_0, \text{M}^{-4} \text{s}^{-1}$	1.238×10^9	$(1.196, 1.280) \times 10^9$



(a) Experimental data vs. proposed model. (b) Parity plot.

Figure 5: (a) Comparison of the proposed model and the model from Guichardon et al.²⁴ for the reaction rate coefficient and the experimental data as a function of the ionic strength. (b) Parity plot showing the calculated values for the reaction rate coefficient and the experimental values. The dashed lines (-) represent $\pm 10\%$ deviation, and the dotted lines (:) represent $\pm 20\%$ deviation, while the dash-dot line (-.) refers to the model from Guichardon et al. The colors and symbols are the same as used in Figure 4.

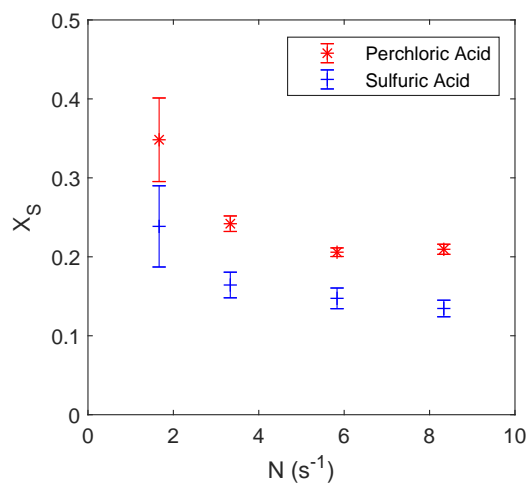
265 3.2 Micromixing experiments

Figure 6 shows the segregation indices obtained from the micromixing experiments. The results from the Stirred Vessel are shown in Figure 6a as a function of stirring speed N . Figure 6b and 6c show the segregation index X_S and X_Q for the Villermaux-Dushman and the second Bourne reaction, respectively, as a function of rotational speed ω in the rotor-stator Spinning Disc Reactor.

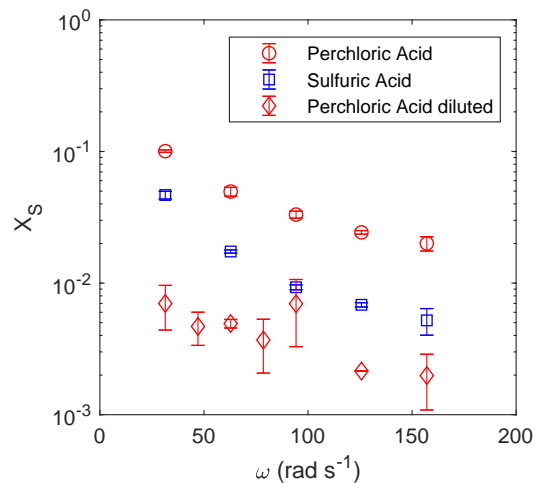
270 These results can be translated into micromixing times by solving the following ordinary differential equations, using the incorporation model¹⁸ or the engulfment model:⁴⁴

$$\frac{dV}{dt} = \frac{V}{t_{mix}}, \quad (28)$$

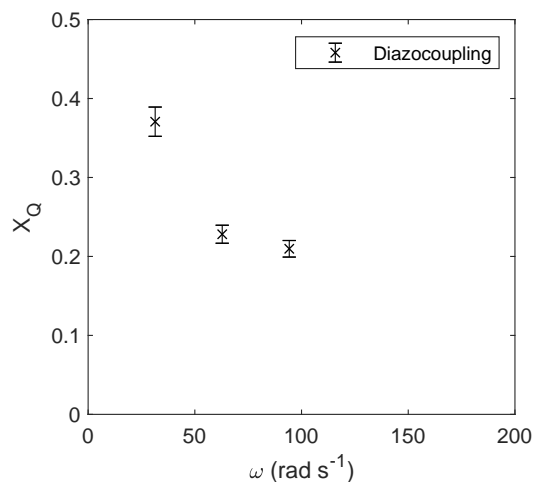
$$\frac{dC_i}{dt} = \frac{(C_{bulk} - C_i)}{t_{mix}} + r_i. \quad (29)$$



(a) SV- Villiermaux Dushman.



(b) rs-SDR - Villiermaux-Dushman.



(c) rs-SDR - Second Bourne reaction.

Figure 6: Segregation index X_S (Villiermaux-Dushman) and X_Q (second Bourne reaction) as a function of the stirring speed N or rotational speed ω for the Stirred Vessel and the rotor-stator Spinning Disc Reactor respectively. Note the logarithmic scale on the y-axis in Figure 6b.

These ODE's model an initial reaction volume that incorporates (or engulfs) liquid from
 275 the surroundings at a rate equal to the inverse value of the micromixing time, allowing
 the reaction to occur inside that growing volume. When the acid is depleted, the final
 concentration of products can be used to calculate the segregation index.

The relationship between micromixing time and segregation index is presented in Figures
 7a and 7b for both systems. It should be noted that full dissociation of sulfuric acid is
 assumed, as it was assumed in the original study by Guichardon et al. as well.²⁴

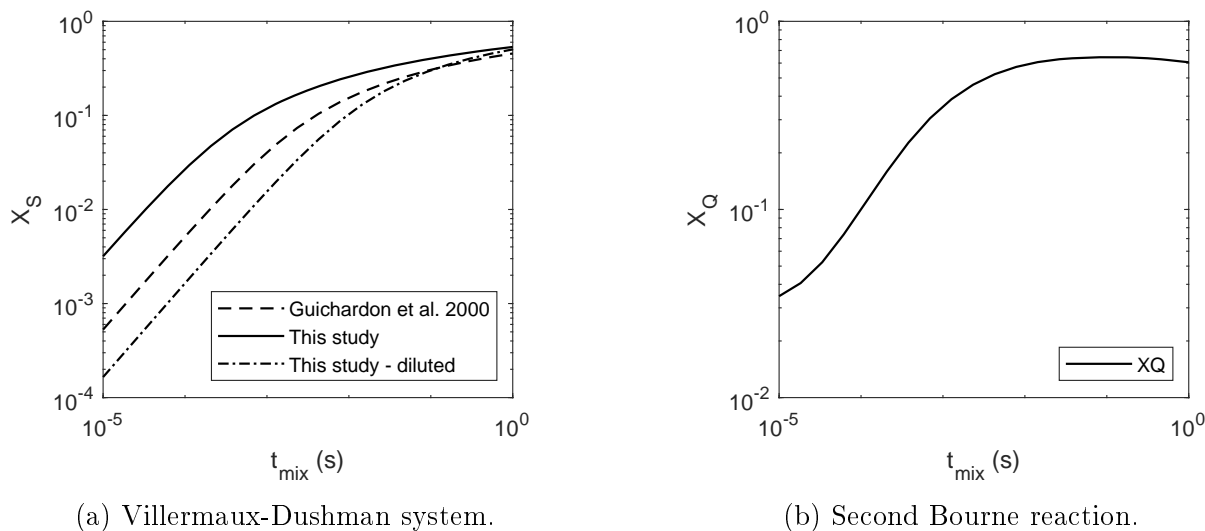


Figure 7: Segregation indices X_S and X_Q versus micromixing time t_{mix} .

280

Micromixing times are presented in Figure 8 as a function of the estimated local energy
 dissipation rate.

4 Discussion

4.1 Experimental results

285

Table 4 compares the reaction rate coefficients from different studies to the ones calculated
 using Equation 26 and 27 with the obtained parameters shown in Table 3. Clearly, the
 results of this kinetic study are in very good agreement with earlier investigations.^{37,53-55} It

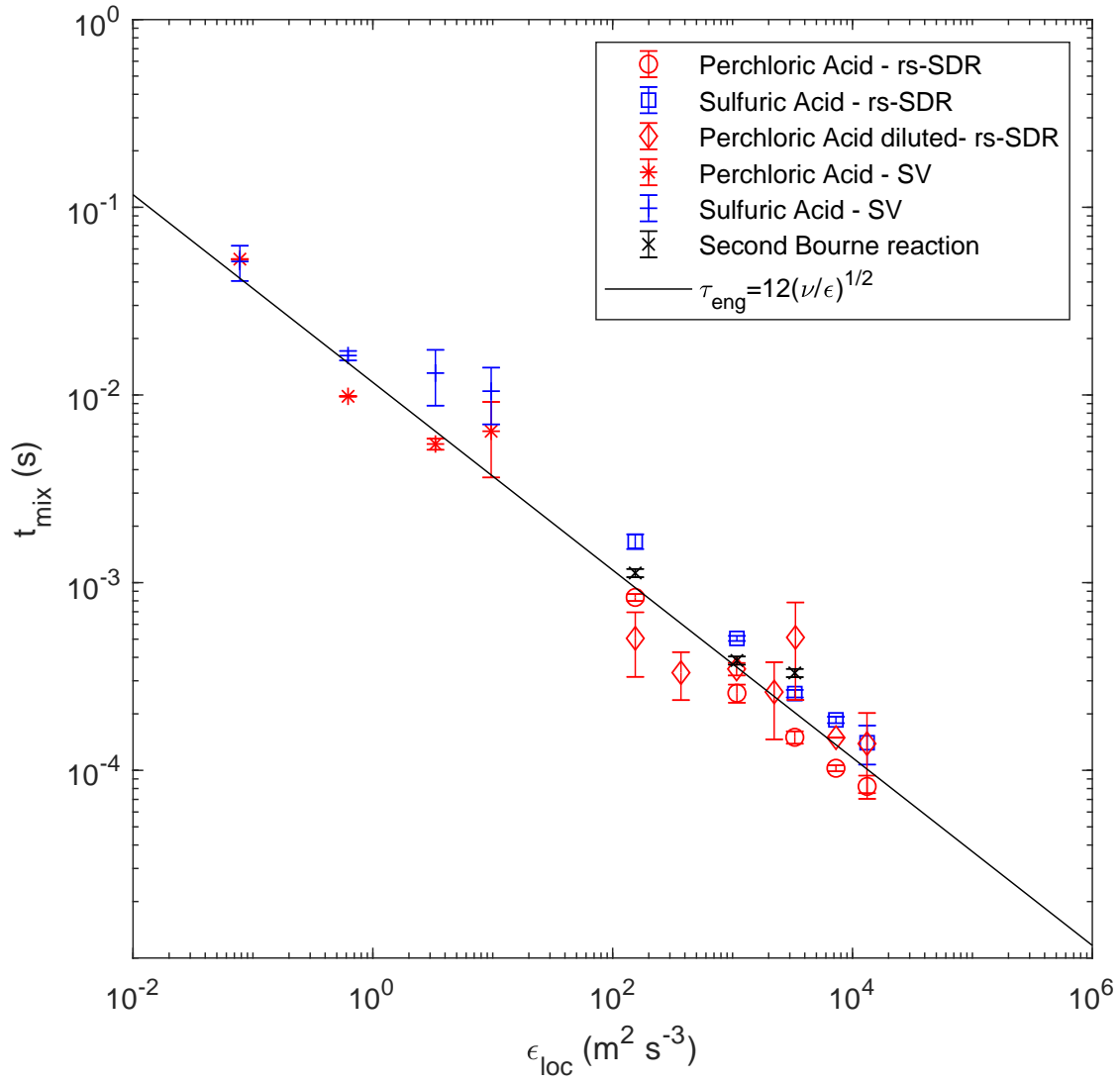


Figure 8: Estimated micromixing time t_{mix} as a function of energy dissipation rate.

is remarkable that at higher values of ionic strength the model proposed by Guichardon et al. underestimates the reaction rate coefficient, deviating as much as one order of magnitude lower than the rest of the reported values. This is very likely due to the incomplete dissociation of sulfuric acid.

Table 4: Comparison of previously published reaction rate coefficients k with those predicted using the kinetic model presented in this study.

I_s , M	Reference	Reported k , $\text{M}^{-4}\text{s}^{-1}$	Calculated k , $\text{M}^{-4}\text{s}^{-1}$ (this study)
0.015	Palmer and Lyons ⁵⁴	6.72×10^8	6.69×10^8
	Schmitz et al. ³⁷	7.19×10^8	
	Guichardon et al. ²⁴	6.80×10^8	
0.1	Palmer and Lyons ⁵⁴	4.27×10^8	3.50×10^8
	Schmitz et al. ³⁷	4.26×10^8	
	Guichardon et al. ²⁴	1.33×10^8	
0.2	Schildcrout and Fortunato ⁵³	3.45×10^8	2.62×10^8
	Schmitz ⁵⁵	3.50×10^8	
	Schmitz et al. ³⁷	3.32×10^8	
	Guichardon et al. ²⁴	5.68×10^7	
1.0	Palmer and Lyons ⁵⁴	2.62×10^8	1.51×10^8
	Barton and Wright ⁵⁶	3.00×10^8	
	Guichardon et al. ²⁴	1.28×10^7	

The experimentally obtained values for k reported by Palmer and Lyons⁵⁴ and Schmitz,⁵⁵ and the k values predicted by the model from Schmitz et al.³⁷ match the experimental results obtained in this study very well. Note that the model from Schmitz et al.³⁷ is limited to $I_s < 0.2$ M.

The effects of incomplete dissociation of sulfuric acid in micromixing experiments have been discussed by other authors,^{26-28,30-32,57} and can be observed in Figure 6a and 6b of this study. Using equivalent proton concentrations and assuming the acids to be fully dissociated, one would expect the same final product distribution. However, this is not the case and the second deprotonation of sulfuric acid appears to be the rate limiting step, based on the lower values of k obtained from the kinetic model from Guichardon et al. and shown in Table 4.

Figure 8 compares the micromixing times obtained by the second Bourne reaction with

those obtained with the Villermaux-Dushman system using both sulfuric acid and perchloric acid in the rs-SDR, and also those obtained in the SV. The micromixing times were calculated using the kinetic model from Guichardon et al.²⁴ for sulfuric acid and using the kinetic model presented in this study for perchloric acid. It is clear that at the investigated acid concentrations of $[H^+] = 1 \text{ M}$ and $[H^+] = 0.1 \text{ M}$, both kinetic models provide similar micromixing times when implemented in the incorporation model. These estimated micromixing times are also close to the theoretical engulfment time proposed by Bałdyga and Bourne⁴³ when the rate of strain of the most active eddy ($12.7\tau_K$) is used as the engulfment parameter.

These results imply that the kinetic model presented in this study can be used for micromixing experiments using perchloric acid and other strong monoprotic acids (a comparison between perchloric acid, hydrochloric acid, nitric acid and sulfuric acid is shown in the Supplementary Information). However, in order to use the kinetic model proposed in this study for experiments performed with sulfuric acid (and other incompletely dissociated acids), additional modeling of the dissociation equilibrium is required. Schmitz et al.³⁷ proposed to include the equilibrium reaction of hydrogen sulfate ions, but the equilibrium constant (taken from Ref.⁵⁸) is only valid for ionic strengths less than 0.3 M, which is not sufficient for the concentrations typically used in micromixing experiments. The kinetic model proposed by Guichardon et al. is therefore only suitable for micromixing experiments using sulfuric acid.

4.2 Limitations

The kinetic model proposed in this study has several limitations that are worth discussing.

First of all and as pointed out by some authors,^{25,26} the concentrations used for the kinetic investigation and the concentrations used for micromixing characterization differ significantly. This issue is somewhat alleviated by the way the incorporation model works, being a reaction volume of concentrated acid that rapidly dilutes by the incorporation of liquid from the surroundings, which at the same time are reacting. As a result, the concentrations in the reacting volume become significantly diluted.

Another limitation is that the fifth order law is introduced as a given in this study.
330 The vast information in the studies from Schmitz et al.^{33-37,55,59} and the early observations
of Palmer et al. and Schildcrout et al.^{53,54} support this assumption. Only at very low
concentrations ($I^- < 10^{-6}$ M) the iodide-iodate reaction shows a different dependency on
the iodide concentration.

In an attempt to tackle these two limitations, Kölbl et al.^{27,57} investigated the partial
335 reaction order of the iodide-iodate system by performing the Villiermaux-Dushman exper-
iments while varying the concentration of the reactants. However, as already pointed out
by Wenzel et al.³² this was more likely caused by chemical attenuation due to the buffer,
since it was kept constant. Furthermore, the different reaction orders observed in different
equipment suggest that the reaction took place under different hydrodynamical conditions
340 rather than the Villiermaux-Dushman method being “instrument dependent”.

Another aspect that requires attention is that all kinetic experiments were executed at
a constant temperature of 20 °C. It was not confirmed whether this model is affected by
increasing temperature. In the work from Palmer et al.,⁵⁴ it was concluded that the effects
of temperature are negligible on the iodide-iodate reaction and only affect the tri-iodide
345 equilibrium.

Finally, it is important to mention that the iodide-iodate reaction in the Villiermaux-
Dushman method requires the assumption of a mechanistic model that represents the course
of mixing and reaction. In this case the incorporation model was assumed. Simple models,
however, cannot describe what exactly occurs in the reaction zone. Direct Numerical Simu-
350 lations are the only possibility to provide better information about hydrodynamics in detail.
Unfortunately, for novel equipment such as the rs-SDR, Rotating Packed Beds, rotor-stator
mixers, etc, the grid size needed to resolve the complex turbulent fields leads to enormous
computational times. Therefore, the use of mixing models and test reactions is still a ne-
cessity to understand the efficiency of chemical reactors. One should consider the order of
355 magnitude of estimated micromixing times for design and scale-up.

5 Conclusions

In this study, a kinetic investigation of the iodide-iodate reaction is presented to improve the quantitative determination of micromixing times when using the Villiermaux-Dushman reaction system. The kinetic experiments are in good agreement with the fifth order rate law
360 for the iodide-iodate reaction. Furthermore, the reaction rate coefficient strongly depended on the ionic strength. A kinetic model is presented that estimates the reaction rate coefficient as a function of the activity of the involved species. A Davies-like expression similar to the one proposed by Bromley was adopted that expresses an overall activity coefficient as a function of ionic strength. The predicted reaction rate coefficients deviated less than 20%
365 from those measured experimentally for most of the experiments.

Micromixing experiments using the Villiermaux-Dushman system with perchloric acid and sulfuric acid were performed in a rotor-stator Spinning Disc Reactor and in an unbaffled Stirred Vessel. Additionally, the second Bourne reaction was performed in the rotor-stator Spinning Disc Reactor. All estimated micromixing times are in line with the theoretical
370 micromixing time as predicted by the engulfment model, using the vorticity of the most active eddy in the turbulent field.

In general, using strong monoprotic acids like perchloric acid is recommended for the Villiermaux-Dushman system, as this prevents uncertainties related to incomplete dissociation of the acid at higher proton concentrations. The kinetic model presented in this study
375 allows accurate estimation of micromixing times when using perchloric acid. In addition, compared to previously published models, our model provides more flexibility thanks to its validity for ionic strengths in the range of $0.003 < I_s < 1$ M.

Acknowledgement

The authors thank Martijn de Belie for starting the comparison of different kinetic models,
380 and Keegan Walker for the experimental work with the second Bourne reaction.

Supporting Information Available

The following files are available:

- Supportive Graph 1: Example of the fitting procedure for the kinetic investigation.
- Supportive Graph 2: Extension of Figure 5a including HCl, HNO₃ and H₂SO₄.

385 References

- (1) Danckwerts, P. The effect of incomplete mixing on homogeneous reactions. *Chemical Engineering Science* **1958**, *8*, 93–102.
- (2) Baldyga, J.; Makowski, Ł.; Orciuch, W. Interaction between Mixing, Chemical Reactions, and Precipitation. *Industrial & Engineering Chemistry Research* **2005**, *44*, 5342–5352.
390
- (3) Villiermaux, J.; Blavier, L. Free radical polymerization engineering-I. A new method for modeling free radical homogeneous polymerization reactions. *Chemical Engineering Science* **1984**, *39*, 87–99.
- (4) Wenzel, D.; Gerdes, N.; Steinbrink, M.; Ojeda, L. S.; Górak, A. Liquid Distribution and Mixing in Rotating Packed Beds. *Industrial & Engineering Chemistry Research* **2019**, 395 *58*, 5919–5928.
- (5) Bourne, J.; Maire, H. Micromixing and fast chemical reactions in static mixers. *Chemical Engineering and Processing: Process Intensification* **1991**, *30*, 23–30.
- (6) Manzano Martínez, A. N.; Van Eeten, K. M.; Schouten, J. C.; Van Der Schaaf, J. Micromixing in a Rotor-Stator Spinning Disc Reactor. *Industrial and Engineering Chemistry Research* **2017**, *56*, 13454–13460.
400

- (7) Chu, G.-W.; Song, Y.-H.; Yang, H.-J.; Chen, J.-M.; Chen, H.; Chen, J.-F. Micromixing efficiency of a novel rotor-stator reactor. *Chemical Engineering Journal* **2007**, *128*, 191–196.
- 405 (8) Jacobsen, N. C.; Hinrichsen, O. Micromixing efficiency of a spinning disk reactor. *Industrial and Engineering Chemistry Research* **2012**, *51*, 11643–11652.
- (9) Chu, G. W.; Song, Y. J.; Zhang, W. J.; Luo, Y.; Zou, H. K.; Xiang, Y.; Chen, J. F. Micromixing efficiency enhancement in a rotating packed bed reactor with surface-modified nickel foam packing. *Industrial and Engineering Chemistry Research* **2015**,
410 *54*, 1697–1702.
- (10) Assirelli, M.; Bujalski, W.; Eaglesham, A.; Nienow, A. Study Of Micromixing in a Stirred Tank Using a Rushton Turbine: Comparison of Feed Positions and Other Mixing Devices. *Chemical Engineering Research and Design* **2002**, *80*, 855–863.
- (11) Baldyga, J.; Bourne, J. R. Interactions between mixing on various scales in stirred tank
415 reactors. *Chemical Engineering Science* **1992**, *47*, 1839–1848.
- (12) Hofinger, J.; Sharpe, R. W.; Bujalski, W.; Bakalis, S.; Assirelli, M.; Eaglesham, A.; Nienow, A. W. Micromixing in two-phase (G-L and S-L) systems in a stirred vessel. *The Canadian Journal of Chemical Engineering* **2011**, *89*, 1029–1039.
- (13) Baldyga, J.; Bourne, J. R.; Yang, Y. Influence of feed pipe diameter on mesomixing in
420 stirred tank reactors. *Chemical Engineering Science* **1993**, *48*, 3383–3390.
- (14) Assirelli, M.; Bujalski, W.; Eaglesham, A.; Nienow, A. W. Intensifying micromixing in a semi-batch reactor using a Rushton turbine. *Chemical Engineering Science* **2005**, *60*, 2333–2339.
- (15) Bourne, J. Mixing on the molecular scale (micromixing). *Chemical Engineering Science*
425 **1983**, *38*, 5–8.

- (16) Baldyga, J.; Pohorecki, R. Turbulent micromixing in chemical reactors - a review. *The Chemical Engineering Journal and The Biochemical Engineering Journal* **1995**, *58*, 183–195.
- (17) Bourne, J. R. Mixing and the Selectivity of Chemical Reactions. *Organic Process Research & Development* **2003**, *7*, 471–508.
- (18) Fournier, M.-C.; Falk, L.; Villiermaux, J. a New Parallel Competing Reaction System for Assessing Micromixing Efficiency—Experimental Approach. *Pergamon Chemical Engineering Science* **1996**, *51*, 5053–5064.
- (19) Bourne, J. R.; Kut, O. M.; Lenzner, J. An improved reaction system to investigate micromixing in high-intensity mixers. *Industrial & Engineering Chemistry Research* **1992**, *31*, 949–958.
- (20) Bourne, J. R.; Kut, O. M.; Lenzner, J.; Maire, H. Kinetics of the diazo coupling between 1-naphthol and diazotized sulfanilic acid. *Industrial & Engineering Chemistry Research* **1990**, *29*, 1761–1765.
- (21) Guichardon, P.; Falk, L. Characterisation of micromixing efficiency by the iodide-iodate reaction system. Part I: experimental procedure. *Chemical Engineering Science* **2000**, *55*, 4233–4243.
- (22) Commenge, J. M.; Falk, L. Villiermaux-Dushman protocol for experimental characterization of micromixers. *Chemical Engineering and Processing: Process Intensification* **2011**, *50*, 979–990.
- (23) Kochkodan, V.; Darwish, N. B.; Hilal, N. *Boron Separation Processes*; 2015.
- (24) Guichardon, P.; Falk, L.; Villiermaux, J. Characterisation of micromixing efficiency by the iodide-iodate reaction system. Part II: Kinetic study. *Chemical Engineering Science* **2000**, *55*, 4245–4253.

- 450 (25) Bourne, J. R. Comments on the iodide/iodate method for characterising micromixing. *Chemical Engineering Journal* **2008**, *140*, 638–641.
- (26) Kölbl, A. Further comments on the Iodide Iodate Reaction Method for characterising micromixing. *Chemical Engineering Journal* **2008**, *145*, 176–177.
- (27) Kölbl, A.; Kraut, M.; Dittmeyer, R. Kinetic investigation of the Dushman reaction
455 at concentrations relevant to mixing studies in microstructured cyclone type mixers. *Chemical Engineering Science* **2013**, *101*, 454–460.
- (28) Guichardon, P.; Ibaseta, N. *Revision of the Dushman Reaction Kinetics for an Improved Micromixing Characterization*.
- (29) Horvath, A. L. A. L.; 1932, *Handbook of aqueous electrolyte solutions : physical prop-*
460 *erties, estimation, and correlation methods*; Ellis Horwood, 1985; p 631.
- (30) Kölbl, A.; Schmidt-Lehr, S. The iodide iodate reaction method: The choice of the acid. *Chemical Engineering Science* **2010**, *65*, 1897–1901.
- (31) Baqueiro, C.; Ibaseta, N.; Guichardon, P.; Falk, L. Influence of reagents choice (buffer, acid and inert salt) on triiodide production in the Villiermaux-Dushman method applied
465 to a stirred vessel. *Chemical Engineering Research and Design* **2018**, *136*, 25–31.
- (32) Wenzel, D.; Assirelli, M.; Rossen, H.; Lopattschenko, M.; Górak, A. On the reactant concentration and the reaction kinetics in the Villiermaux-Dushman protocol. *Chemical Engineering and Processing - Process Intensification* **2018**, *130*, 332–341.
- (33) Schmitz, G. Inorganic reactions of iodine(+1) in acidic solutions. *International Journal of Chemical Kinetics* **2004**, *36*, 480–493.
470
- (34) Schmitz, G. Inorganic reactions of iodine(III) in acidic solutions and free energy of iodous acid formation. *International Journal of Chemical Kinetics* **2008**, *40*, 647–652.

- (35) Schmitz, G. Iodine oxidation by hydrogen peroxide in acidic solutions, Bray-Liebhafsky reaction and other related reactions. *Physical Chemistry Chemical Physics* **2010**, *12*, 6605.
475
- (36) Schmitz, G. Iodine oxidation by hydrogen peroxide and Bray-Liebhafsky oscillating reaction: effect of the temperature. *Phys. Chem. Chem. Phys* **2011**, *13*, 7102–7111.
- (37) Schmitz, G.; Bourceanu, G.; Ungureanu, I. Effects of Ce(III) and Mn(II) on the Dushman reaction and simulations of the Briggs-Rausher reaction. *Reaction Kinetics, Mechanisms and Catalysis* **2018**, *123*, 81–92.
480
- (38) Manzano Martínez, A. N.; Haase, A. S.; Assirelli, M.; van der Schaaf, J. An improved kinetic model for micromixing characterization using the Villiermaux-Dushman method. 2019 AIChE Annual Meeting proceedings.
- (39) Myers, O. E. Kinetics of the triiodide equilibrium. *The Journal of Chemical Physics*
485 **1958**, *28*, 1027–1029.
- (40) Palmer, D. A.; Ramette, R. W.; Mesmer, R. E. Triiodide ion formation equilibrium and activity coefficients in aqueous solution. *Journal of Solution Chemistry* **1984**, *13*, 673–683.
- (41) Coblenz, V. *A Manual of Volumetric Analysis: Treating on the Subjects of Indicators, Test-papers, Alkalimetry, Acidimetry, Analysis by Oxidation and Reduction, Iodometry, Assay Processes for Drugs with the Titrimetric Estimation of Alkaloids, Estimation of Phenol, Sugar, Tables of Atomic and Molecular Weights*; P. Blakiston's Son, 1901.
490
- (42) Kolmogorov, A. N. The Local Structure of Turbulence in Incompressible Viscous Fluid for Very Large Reynolds Numbers. *Proceedings of the Royal Society A: Mathematical, Physical and Engineering Sciences* **1991**, *434*, 9–13.
495
- (43) Baldyga, J.; Bourne, J. R. *Turbulent mixing and chemical reactions*; Wiley, 1999.

- (44) Baldyga, J.; Bourne, J. R. Simplification of micromixing calculations. I. Derivation and application of new model. *The Chemical Engineering Journal* **1989**, *42*, 83–92.
- (45) Assirelli, M.; Bujalski, W.; Eaglesham, A.; Nienow, A. W. Macro- and micromixing studies in an unbaffled vessel agitated by a Rushton turbine. *Chemical Engineering Science* **2008**, *63*, 35–46.
- (46) Lee, K. C.; Yianneskis, M. Turbulence Properties of the Impeller Stream of a Rushton Turbine. *AIChE Journal* **1998**, *44*, 13–24.
- (47) Sharp, K. V.; Adrian, R. J. PIV Study of small-scale flow structure around a Rushton turbine. *AIChE Journal* **2001**, *47*, 766–778.
- (48) Ng, K.; Yianneskis, M. Observations on the distribution on energy dissipation in stirred vessels. *Chemical Engineering Research and Design*. 2000.
- (49) Armenante, P. M.; Luo, C.; Chou, C. C.; Fort, I.; Medek, J. Velocity profiles in a closed, unbaffled vessel: Comparison between experimental LDV data and numerical CFD predictions. *Chemical Engineering Science* **1997**,
- (50) Daily, J. W.; Nece, R. E. Chamber Dimension Effects on Induced Flow and Frictional Resistance of Enclosed Rotating Disks. *Journal of Basic Engineering* **1960**, *82*, 217.
- (51) de Beer, M.; Keurentjes, J.; Schouten, J.; van der Schaaf, J. Bubble formation in co-fed gas–liquid flows in a rotor-stator spinning disc reactor. *International Journal of Multiphase Flow* **2016**, *83*, 142–152.
- (52) Bromley, L. A. Thermodynamic properties of strong electrolytes in aqueous solutions. *AIChE Journal* **1973**, *19*, 313–320.
- (53) Schildcrout, S. M.; Fortunato, F. A. Spectrophotometric study of the rate of the aqueous iodate-iodide reaction. *The Journal of Physical Chemistry* **1975**, *79*, 31–34.

- 520 (54) Palmer, D.; Lyons, L. *Kinetics of iodine hydrolysis in unbuffered solutions*; 1989.
- (55) Schmitz, G. Kinetics and mechanism of the iodate-iodide reaction and other related reactions. *Physical Chemistry Chemical Physics* **1999**, *1*, 1909–1914.
- (56) Barton, A. F. M.; Cheong, H. N.; Smidt, R. E. Kinetics of the bromate-iodide and iodate-iodide reactions by pH-stat techniques. *Journal of the Chemical Society, Faraday Transactions 1: Physical Chemistry in Condensed Phases* **1976**, *72*, 568.
- 525 (57) Kölbl, A.; Desplantes, V.; Grundemann, L.; Scholl, S. Kinetic investigation of the Dushman reaction at concentrations relevant to mixing studies in stirred tank reactors. *Chemical Engineering Science* **2013**,
- (58) Clegg, S. L.; Rard, J. A.; Pitzer, K. S. Thermodynamic properties of 0-6 mol kg⁻¹ aqueous sulfuric acid from 273.15 to 328.15 K. *J. Chem. Soc., Faraday Trans.* **1994**,
- 530 *90*, 1875–1894.
- (59) Schmitz, G. Kinetics of the Dushman reaction at low I⁻ concentrations. *Physical Chemistry Chemical Physics* **2000**, *2*, 4041–4044.

List of Figures

535	1	Schematic representation of the batch setup used for the kinetic study	7
	2	Schematic representation of the rotor-stator spinning disc reactor used for the micromixing experiments.	13
	3	Schematic representation of the Stirred Vessel used for the micromixing experiments.	13
540	4	Reaction rate coefficient k as function of the specified parameters for the experimental conditions summarized in Table 1. Error bars represent the standard deviation for at least three experiments.	16

5	(a) Comparison of the proposed model and the model from Guichardon et al. ²⁴ for the reaction rate coefficient and the experimental data as a function of the ionic strength. (b) Parity plot showing the calculated values for the reaction rate coefficient and the experimental values. The dashed lines (-) represent $\pm 10\%$ deviation, and the dotted lines (:) represent $\pm 20\%$ deviation, while the dash-dot line (-.) refers to the model from Guichardon et al. The colors and symbols are the same as used in Figure 4.	18
545		
6	Segregation index X_S (Villermoux-Dushman) and X_Q (second Bourne reaction) as a function of the stirring speed N or rotational speed ω for the Stirred Vessel and the rotor-stator Spinning Disc Reactor respectively. Note the logarithmic scale on the y-axis in Figure 6b.	19
550		
7	Segregation indices X_S and X_Q versus micromixing time t_{mix}	20
8	Estimated micromixing time t_{mix} as a function of energy dissipation rate. . .	21
555		

Graphical TOC Entry

